



Overview and introduction to development of non-ergodic earthquake ground-motion models

Grigorios Lavrentiadis¹ · Norman A. Abrahamson² · Kuehn M. Nicolas¹ · Yousef Bozorgnia³ · Christine A. Goulet⁴ · Anže Babič⁵ · Jorge Macedo⁶ · Matjaž Dolšek⁵ · Nicholas Gregor⁷ · Albert R. Kottke⁸ · Maxime Lacour⁹ · Chenying Liu⁶ · Xiaofeng Meng⁴ · Van-Bang Phung¹⁰ · Chih-Hsuan Sung¹⁰ · Melanie Walling¹¹

Received: 11 November 2021 / Accepted: 20 July 2022 / Published online: 17 August 2022
© The Author(s) 2022

Abstract

This paper provides an overview and introduction to the development of non-ergodic ground-motion models, GMMs. It is intended for a reader who is familiar with the standard approach for developing ergodic GMMs. It starts with a brief summary of the development of ergodic GMMs and then describes different methods that are used in the development of non-ergodic GMMs with an emphasis on Gaussian process (GP) regression, as that is currently the method preferred by most researchers contributing to this special issue. Non-ergodic modeling requires the definition of locations for the source and site characterizing the systematic source and site effects; the non-ergodic domain is divided into cells for describing the systematic path effects. Modeling the cell-specific anelastic attenuation as a GP, and considerations on constraints for extrapolation of the non-ergodic GMMs are also discussed. An updated unifying notation for non-ergodic GMMs is also presented, which has been adopted by the authors of this issue.

Keywords Probabilistic seismic hazard analysis · Non-ergodic ground-motion model · Gaussian process regression

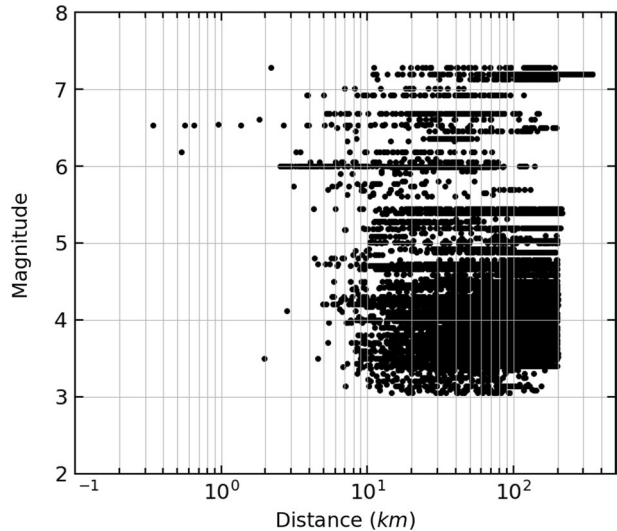
1 Introduction

Due to the limited number of ground-motion recordings in a region, the traditional approach to developing ground-motion models (GMMs) for use in probabilistic seismic hazard analysis (PSHA) has been to combine data from similar tectonic environments around the world together and develop a model for the scaling with magnitude, distance, and site conditions. The median and aleatory variability of a GMM are assumed to be applicable to any location within the broad tectonic category. This is known as the ergodic assumption in ground-motion modeling (Anderson and Brune 1999).

✉ Grigorios Lavrentiadis
glavrentiadis@ucla.edu

Extended author information available on the last page of the article

Fig. 1 Magnitude-distance distribution of the California subset of the NGAWest2 dataset



The traditional approach of developing ergodic GMMs leads to a stable global average of the ground motion for a given scenario, but a large aleatory variability between an observation and the global average. With the large increase in the number of ground-motion instruments and recordings over the last decade, it has become clear that there are significant systematic differences in ground motion based on the location of the site and the source. As a result, the ergodic GMMs generally may not work well for a specific site/source location. This has prompted the development of non-ergodic ground-motion models in which these location-specific effects are modeled explicitly, which reduces the aleatory variability. The uncertainty in the estimate of the site-specific effects is then part of the epistemic uncertainty. As a general classification, uncertainties are treated as epistemic if they are expected to be reduced by gathering more data. Variabilities are treated as aleatory if the increase of data is not expected to systematically reduce their range (Der Kiureghian and Ditlevsen 2009).

An important difference between the application of statistics in GMMs as compared to most other fields is the use of constraints to ensure proper extrapolation. In other fields, the assumption is that the key behaviors are represented by the available data. Thus, the goal of statistics is to find the trends in the data. However, the problem is more complicated in GMMs as they are often applied to earthquake scenarios outside the range that is well constrained by the data (i.e., it is an extrapolation problem). For instance, Fig. 1 shows the magnitude-distance distribution of the California subset of the NGA-West2 database (Ancheta et al. 2014), which is often used for the development of GMMs for California. In this dataset, the magnitudes range from 3 to 7.2, with the majority of the events being between magnitude 3 and 5, and the distance ranges from 1 to 400 km, with the majority of the recordings being between 20 and 200 km. However, in PSHA, large-magnitude and short-distance scenarios often control the hazard. For example, in the San Francisco Bay Area, it is common to have faults that are less than 10 km away from a site and are capable of producing larger than $M7$ earthquakes. It is the difference between the range of the scenarios that are used to derive a GMM and the

range of scenarios on which a GMM is applied that makes the proper extrapolation of the ground motion an important aspect of a GMM.

This paper serves as an overview and introduction to the development of non-ergodic GMMs, with an emphasis on the varying coefficient models (VCM) developed with Gaussian processes (GPs) regression. The combination of a VCM GMM with the cell-specific anelastic attenuation and considerations regarding the extrapolation of non-ergodic GMMs are also discussed. An updated notation for key elements of non-ergodic GMMs is also presented.

2 Proposed notation

The proposed notation is intended to help the reader understand the role of different terms in a GMM and facilitate the comparison of the different non-ergodic models in this special issue.

The model variables are categorized into two groups: the model parameters (θ) and model hyperparameters (θ_{hyp}). The θ includes the ergodic and non-ergodic terms that directly affect the ground motion, while θ_{hyp} includes the set of variables that control the behavior of the ergodic and non-ergodic terms and have an indirect effect on the ground motion. An example of a model parameter is the coefficient for the linear magnitude scaling, and an example of a hyperparameter is the between-event standard deviation.

The ergodic coefficients of the GMM are denoted as c_i where i is the number of the ergodic term, and the non-ergodic coefficients are denoted as $c_{i,X}$ or $\delta c_{i,X}$. The subscript X (subscript after the comma) can be the letters E , P , or S depending on whether the non-ergodic coefficient in question is intended to capture systematic effects related to the source (earthquake), path, or site. The notation δ is used to differentiate between non-ergodic coefficients that have a zero mean and act as adjustments to ergodic coefficients, and stand-alone non-ergodic coefficients that encompass both the average scaling and the systematic effects. For instance, the non-ergodic term $\delta c_{1,E}$ acts on top of c_1 to capture the systematic effects related to the source. Alternatively, the same behaviour can be modeled with $c_{1,E}$ which is equal to the sum of the ergodic coefficient and the non-ergodic adjustment ($c_{1,E} = c_1 + \delta c_{1,E}$). The non-ergodic adjustments, $\delta c_{i,X}$, are typically used when a non-ergodic GMM is developed with an ergodic GMM as a "backbone" model, in which case the non-ergodic adjustments are estimated based on the total ergodic residuals. For example, Kuehn et al. (2019) and Lavrentiadis et al. (2021) are non-ergodic GMMs derived with this approach. The non-ergodic coefficients, $c_{i,X}$, are used when a non-ergodic GMM is directly estimated with the log of the ground motion as a response variable as in the case of Landwehr et al. (2016).

Many of the non-ergodic GMMs in this issue used the cell-specific anelastic attenuation, first proposed by Dawood and Rodriguez-Marek (2013), to model the systematic path effects. In the proposed notation, the vector of attenuation coefficients of all the cells is denoted as $\mathbf{c}_{ca,P}$, and cell path segments are denoted as $\Delta \mathbf{R}$. The total anelastic attenuation is equal to $\mathbf{c}_{ca,P} \cdot \Delta \mathbf{R}$.

The terms $\delta L2L$, $\delta P2P$, and $\delta S2S$ introduced by Al Atik et al. (2010) are used here to describe the total non-ergodic effects related to the source (they used L for location), path, and site, respectively. For instance, if the constant c_1 is modified by two site adjustments, $\delta c_{1a,S}$ and $\delta c_{1b,S}$, to express the systematic site effects, then $\delta S2S$ is equal to $\delta c_{1a,S} + \delta c_{1b,S}$. Similarly, if the non-ergodic adjustment to the geometrical spreading coefficient, $\delta c_{3,P}$, and

the cell-specific anelastic attenuation, $\mathbf{c}_{ca,P}$ are used to express the systematic path effects, then $\delta P2P = \ln(R)\delta c_{3,P} + \mathbf{c}_{ca,P} \cdot \Delta \mathbf{R} - c_7 R_{rup}$, where, in this example, c_7 is the ergodic anelastic attenuation coefficient. The $c_7 R_{rup}$ term is subtracted from the median prediction from the GMM to remove the systematic effects that are included in the cell-specific anelastic attenuation.

The scale and correlation length which control the spatial distribution of the non-ergodic terms are denoted as $\omega_{i,X}$ and $\ell_{i,X}$. An in-depth discussion on modeling the non-ergodic terms as GPs, where $\omega_{i,X}$ and $\ell_{i,X}$ are defined, is provided in Sect. 5.1. In keeping with the Al Atik et al. (2010) notation, the total epistemic uncertainty of the non-ergodic source, path, and site effects are denoted as τ_{L2L} , ϕ_{P2P} , and ϕ_{S2S} . Expanding from the example above, if $\omega_{1a,S}$ and $\omega_{1b,S}$ correspond to the scales of $\delta c_{1a,S}$ and $\delta c_{1b,S}$, then the epistemic uncertainty of the site effects is $\phi_{S2S}^2 = \omega_{1a,S}^2 + \omega_{1b,S}^2$.

The response variable of the regression is denoted as y . For a pseudo-spectral acceleration (PSA) or Effective Amplitude Spectrum (EAS) GMM, y is equal to $\ln(\text{PSA})$ or $\ln(\text{EAS})$.

The location of the source, site, etc. are required in the non-ergodic GMMs included in this issue to define the spatially-varying non-ergodic terms. The coordinates of the earthquake, site, and mid-point between the source and site are denoted as: t_E , t_S , t_{MP} , respectively. The definition of the location of the earthquake, t_E (e.g. epicenter, the closest point to the site, etc.) is defined in each study. Similarly, the cell coordinates are denoted as t_C ; the exact point of the cell (e.g. center, lower left corner, etc.) to which t_C corresponds is defined in each study.

The star superscript is used to denote the new scenarios and values of non-ergodic coefficients predicted for the new scenarios. For instance, t_E^* corresponds to the source locations of the new scenarios where systematic source effects will be predicted, and $\delta c_{i,E}^*(t_E^*)$ corresponds to the non-ergodic source adjustments of these scenarios.

A list of abbreviations and a glossary of all terms used in this special issue are provided at the end of this paper.

3 Development of ergodic ground-motion models

A typical GMM has a model for the base magnitude, distance, and linear site scaling, and may include more complicated features for non-linear site response, hanging-wall effects, basin effects, etc. For example, the median for the ASK14 (Abrahamson et al. 2014) GMM has the following form:

$$\begin{aligned}
 f_{erg}(M, R_{rup}, V_{S30}, \dots) = & c_1 + c_2 M + c_3 (8.5 - M)^2 + (c_4 + c_5 M) \ln(R_{rup} + c_6) + c_7 R \\
 & + c_8 F_{RV} + c_9 F_N + c_{10} \ln(V_{S30}/V_{ref}) \\
 & + f_{NL}(V_{S30}, z_{1100}) + f_{HW}(M, R_{rup}, R_x, Dip)
 \end{aligned}
 \tag{1}$$

where f_{erg} is the function for the ergodic median ground-motion, c_i are the ergodic scaling coefficients, F_{RV} and F_N are the reverse and normal fault scaling factors, f_{NL} is the non-linear site effects scaling, f_{HW} is the hanging wall scaling, M is the moment magnitude, R_{rup} is the closest distance to the rupture plane, R_x is the horizontal distance from the top edge of the rupture measured perpendicular to the fault strike, V_{S30} is the time-average shear wave velocity at the top 30 m, V_{ref} is the reference V_{S30} for the linear site amplification, z_{1100} is the depth to 1100 m/sec shear-wave velocity, and Dip is the fault dip angle.

C are equal to $\tau^2 + \phi^2$, the off-diagonal elements that are associated with recordings of the same earthquake are equal to τ^2 , and the remaining elements are equal to zero.

Maximum likelihood regressions are computationally inexpensive, as there are efficient methods to minimize the negative of the log-likelihood (e.g. Bound Optimization BY Quadratic Approximation (BOBYQA), Powell (2009)). The most involved step at each iteration is the calculation of the inverse of the covariance matrix; however, due to its block diagonal and sparse nature, the process is computationally efficient to perform.

3.2 Other methods for ergodic models

Ergodic GMMs have also been developed using Bayesian regression. Bayesian models have been used successfully in the development of a *FAS* GMM for Mexico City (Ordaz et al. 1994), in deriving a *PSA* GMM that includes the correlation between spectral periods and the correlation between the GMM coefficients (Arroyo and Ordaz 2010a, b), in capturing the uncertainty of model parameters, such as V_{S30} (Kuehn and Abrahamson 2018), and in the development of ergodic GMMs with truncated data (Kuehn et al. 2020). More closely related to the non-ergodic GMMs of this special issue, Hermkes et al. (2014) used a Bayesian GP regression to derive a non-parametric ergodic GMM for shallow crustal events. Bayesian regression has a higher computational cost than MLE which is why it is less commonly used in GMM development.

GMMs have also been derived through artificial neural networks (ANNs). Derras et al. (2014) proposed an ANN that partitions the residuals into within-event and between-event terms and used it to develop an ergodic GMM for Europe. Withers et al. (2020) applied an ANN to develop an ergodic GMM with ground motions from the CyberShake simulations for Southern California. This is a promising approach, especially for large databases, as the method scales well to many GBs of data that are frequently produced from simulation outputs ($> 10^8$ records). However, extra prudence is required as the modeler does not have direct control over the model behavior (such as interdependency among input terms) which may limit the accurate extrapolation outside the range of training predictor variables. These concerns can be mitigated by applying physics-based constraints on the model or by augmenting the empirical dataset with synthetic datasets, however, this approach requires additional validation to ensure that conditions within the synthetic ground motions are consistent with empirical records and do not introduce any inherent bias within the data.

4 Development of partially non-ergodic ground-motion models

The term “partially non-ergodic” has sometimes been used for GMMs that include mean regional differences. Here, we use the term only for GMMs that include differences due to the location of the site and/or the location of the source, not for average differences between broad regions. One such partially non-ergodic GMM approach consists of capturing systematic (i.e., site-specific) site effects (Stewart et al. 2017). Every site has its own velocity profile which leads to a repeatable site amplification relative to the reference profile of a GMM for the same V_{S30} (Lavrentiadis 2021). This amplification is the same for all ground motions at the site of interest and is not applicable to different sites. However, in an ergodic model, any misfit between a ground-motion observation and the median ground-motion estimate is considered aleatory in nature (i.e. random). That is, ergodic GMMs are based on an assumption that the range of site amplification between different sites with the same V_{S30} is the same as the range

of site amplification at the site of interest. It is the goal of partially non-ergodic GMM to properly categorize the systematic site-specific site amplification effects and remove them from the aleatory terms.

In the partially non-ergodic model, the ergodic within-event residual is partitioned into a site-specific site term and the new remaining within-event within-site residual (δWS_{es}). Using the Al Atik et al. (2010) notation:

$$\delta W_{es} = \delta S2S_s + \delta WS_{es} \tag{5}$$

$\delta S2S_s$ term represents the systematic difference between the site amplification at the s^{th} site and the site amplification in the ergodic GMM.

The parameters of a partially non-ergodic GMM can be formulated as a mixed-effects model with three random terms (δB_e , δWS_{es} , and $\delta S2S_s$):

$$y_{es} = f_{erg}(M, R, V_{S30}, \dots) + \delta S2S_s + \delta B_e + \delta WS_{es} \tag{6}$$

δB_e , δWS_{es} , $\delta S2S_s$ are assumed to be normally distributed with zero means and τ_0 , ϕ_{SS} , and ϕ_{S2S} standard deviations, respectively. This leads to a more complicated covariance matrix with more non-zero off-diagonal terms:

$$\begin{aligned} \mathbf{C} &= \phi_{SS}^2 \mathbf{I}_N + \phi_{S2S}^2 \sum_{i=1}^{N_s} \mathbf{1}_{n_i} + \tau_0^2 \sum_{i=1}^{N_e} \mathbf{1}_{n_i} \\ &= \begin{bmatrix} \phi_{SS}^2 + \phi_{S2S}^2 + \tau_0^2 & \tau_0^2 & \phi_{S2S}^2 & 0 \\ \tau_0^2 & \phi_{SS}^2 + \phi_{S2S}^2 + \tau_0^2 & 0 & \phi_{S2S}^2 \\ \phi_{S2S}^2 & 0 & \phi_{SS}^2 + \phi_{S2S}^2 + \tau_0^2 & \phi_{S2S}^2 \\ 0 & \phi_{S2S}^2 & \tau_0^2 & \phi_{SS}^2 + \phi_{S2S}^2 + \tau_0^2 \end{bmatrix} \end{aligned} \tag{7}$$

The main difference to the covariance matrix of the ergodic GMM (Eq. 4) is that the elements that are associated with the same station include the ϕ_{S2S}^2 variance. In this framework, $\sqrt{\tau_0^2 + \phi_{S2S}^2}$ is the aleatory variability of the GMM, and, ϕ_{S2S} is the epistemic uncertainty of the site term at a site without site-specific data to constrain the site term.

Alternatively, $\delta S2S_s$ can be estimated directly by partitioning the ergodic within-event residuals, δW_{es} , into $\delta S2S_s$ and δWS_{es} . This approach is expected to give similar results, but it can be problematic if some of the systematic site effects have been mapped into the ergodic event terms.

The $\delta S2S_s$ of such a partially non-ergodic GMM is spatially independent. This is a contrast with the GP-based approach (Sect. 5.1), which allows for $\delta S2S_s$ to be spatially correlated.

5 Development of non-ergodic ground-motion models

The fully non-ergodic GMM extends the partially non-ergodic GMM to account for systematic and repeatable source and path effects in addition to the systematic site effects. For that, two additional non-ergodic terms are added:

$$y_{es} = f_{erg}(M, R_{rup}, V_{S30}, \dots) + \delta S2S_s + \delta P2P_{es} + \delta L2L_e + \delta B_e^0 + \delta WS_{es}^0 \tag{8}$$

The $\delta L2L_e$ term is the systematic source-specific adjustment to the median ground motion in the base ergodic model. It is related to repeatable effects in the release of seismic energy from a source in a region. For instance, $\delta L2L_e$ will be positive if the average stress drop

of earthquakes in a region (i.e. fault system) is systematically larger than the global average. Supporting this argument, Trugman and Shearer (2018) found a strong correlation between the stress drop and between-event term of an ergodic GMM. Similarly, the $\delta P2P_{es}$ term represents the repeatable difference in the propagation of the seismic waves between a source and site and the ergodic GMM. The $\delta P2P_{es}$ term will be positive if the attenuation in a geographical region is less than the global average.

The non-ergodic terms $\delta L2L_e$ and $\delta P2P_{es}$ are assumed to be normally distributed with zero means and τ_{L2L} and ϕ_{P2P} standard deviation, respectively. The remaining aleatory terms, δB_e^0 and δWS_{es}^0 , are assumed to be normally distributed with zero means and τ_0 and ϕ_0 standard deviations.

The different GMM paradigms (e.g. ergodic, partially non-ergodic, and fully non-ergodic GMMs) should have similar size total aleatory variability and epistemic uncertainty: $\sqrt{\phi^2 + \tau^2} \approx \sqrt{\phi_{S2S}^2 + \phi_{SS}^2 + \tau^2} \approx \sqrt{\tau_{L2L}^2 + \phi_{P2P}^2 + \phi_{S2S}^2 + \phi_0^2 + \tau_0^2}$ as there is no change in the amount of information—what is different between the three approaches is how the provided information is treated (i.e. repeatable or random). This is a useful check for ensuring that the epistemic uncertainty and aleatory variability of a GMM are not overestimated or underestimated. However, it should be noted that the size of aleatory variability and epistemic uncertainty also depends on the modeling approach. For example, a single-station partially non-ergodic GMM, such as SWUS15 (Abrahamson et al. 2015) has, largely, a constant epistemic uncertainty, whereas, a non-ergodic GMM developed as GP has a scenario-dependent epistemic uncertainty. Therefore, this check is primarily applicable at the center of the ground motion data, not at the model extrapolation.

Lin et al. (2011) estimated the standard deviations for all three non-ergodic terms using ground-motion data from Taiwan. The $\delta S2S_s$ was modeled as a random term based on the site ID, and $\delta L2L_e$ was modeled as a spatially correlated random variable based on the site location using standard geostatistics. A more complex spatial correlation model was used for $\delta P2P_{es}$, as it depends both on the source and site location. For a single site, the $\delta P2P_{es}$ correlation is stronger if the earthquakes are closer together, as the seismic waves travel through the same part of the crust. The systematic path effects were found to result in the largest reduction of the aleatory variability followed by the systematic site effects. Overall, including all three effects led to about a 40% reduction in the total aleatory standard deviation compared to the ergodic GMM.

In the previous formulation, the non-ergodic effects were modeled with normal distributions, which may not always be appropriate, particularly, for the path terms; for similar variations in the attenuation of the earth's crust, a far apart source-site pair will have more pronounced path effects than a source-site pair that is closer together. The distance dependence of the path effects is not significant if all records in the dataset have similar rupture distances, but it can be important if the range of R_{rup} is large.

An alternative option is to describe the non-ergodic GMM as a varying coefficient model (VCM). In this approach, the non-ergodic terms are scaled by different model variables (e.g. R_{rup} , V_{S30}) which provides a more flexible framework to model the systematic effects. More details on the development of non-ergodic GMMs as GP VCMs are provided in the next section.

5.1 Gaussian process models

The non-ergodic GMMs in this special issue are classified as VCM, as the non-ergodic terms are dependent on the earthquake and site locations in addition to any other input parameters (e.g. V_{S30}):

$$\begin{aligned}
 y_{es} &= f_{nerg}(M, R_{rup}, V_{S30}, \dots, t_S, t_E) + \delta B_e^0 + \delta WS_{es}^0 \\
 &= f_{erg}(M, R_{rup}, V_{S30}, \dots) + \delta S2S(V_{S30}, \dots, t_S) + \delta P2P(R_{rup}, \dots, t_E, t_S,) \\
 &\quad + \delta L2L(M, \dots, t_E) + \delta B_e^0 + \delta WS_{es}^0
 \end{aligned}
 \tag{9}$$

with f_{nerg} corresponding to the function of the median non-ergodic ground motion for a particular pair of source and site, while f_{erg} is the function of the median ergodic ground motion (i.e. the median ground motion for all sources and sites). The systematic source term, $\delta L2L$, is modeled as a function of the earthquake coordinates (t_E), and the systematic site term, $\delta S2S$, is modeled as a function of the site coordinates (t_S). The systematic path term, $\delta P2P$, is more complex as it depends both on the earthquake and site location. The cell-specific anelastic attenuation which is used to capture the systematic path effects is described in Sect. 5.1.3.

At first sight, the development of a non-ergodic VCM GMM may seem futile due to the large number of non-ergodic terms that need to be estimated. If the state of California is broken into a 5×5 km grid, there would be approximately 20,000 grid points and so, at minimum, 60,000 non-ergodic coefficients that would need to be estimated; that is the simplest non-ergodic model where the systematic source, site, and path effects are captured with one coefficient each. It is unfeasible to derive such a model with the existing datasets as they contain, at best, in the order of 10,000 recordings. Fortunately, this is not a problem in VCM due to the spatial correlation structure imposed on the non-ergodic coefficients.

In the statistical approaches described so far, the GMM coefficients are treated as fixed parameters. That is, every coefficient has a single value which is estimated by the MLE or another frequentist approach. In a GMM that is developed as a VCM GP, the model coefficients are treated as random variables that are assumed to follow Normal (Gaussian) distributions. The choice of the mean and covariance function of these distributions is what controls the behavior of each coefficient; for instance, whether a coefficient is constant over a domain, whether it varies continuously on some finite length scale, or whether it is spatially independent (i.e. the value of the coefficient at some location is independent of the value of the coefficient at some other location). In this sense, in a GP regression, the GMM coefficients are modeled similarly to the aleatory terms in the mixed-effects regression (Sect. 3.1). It is these constraints on the GMM coefficients imposed by the covariance function that make the development of a non-ergodic VCM GP GMM tractable. Due to this, the non-ergodic GMM coefficients do not have to be estimated directly; instead, only the hyperparameters that control the distributions of the non-ergodic terms need to be estimated by the regression. With the current size of datasets, the number of hyperparameters is typically about 10.

Furthermore, this formulation leads to a scenario-dependent epistemic uncertainty that is more appropriate than the constant epistemic uncertainty assumed in earlier studies. In a VCM GP GMM, the non-ergodic coefficients have a constant epistemic uncertainty, but the epistemic uncertainty of the ground motion is scaled by the GMM input variables. For example, consider a non-ergodic GMM based on the base model (Eq. 1) where the systematic path effects are modeled with a spatially varying geometrical spreading coefficient that is

a function of the earthquake coordinates ($c_{4,E}(t_E)$). In this case, the epistemic uncertainty of $c_{4,E}(t_E)$ will be equal to $\psi_{4,E}(t_E)$ and the epistemic uncertainty of the ground motion due to the systematic path effects will be equal to $\phi_{P2P} = \psi_{4,E}(t_E) \ln(R + c_6)$. This results in a distance-dependent epistemic uncertainty, the epistemic uncertainty is higher for sites farther from the source, which is different from the ϕ_{P2P} values of Lin et al. (2011) which are independent of the source-to-site distance.

GP is a particular case of a hierarchical Bayesian model as it is expressed on multiple levels. At the base level are the GMM coefficients and aleatory terms which have a direct impact on the response variable y and are defined in terms of some distributions; the variables that constitute this level are called model parameters (θ). At the next level is the set of variables that control the distributions of θ . The variables of the upper level are called model hyperparameters (θ_{hyp}), which in turn could be defined in terms of some other distributions or they could be fixed. As an example, in this context, ϕ_0 and τ_0 are hyperparameters that control the distributions of the parameters: δWS_{es}^0 and δB_e^0 .

There are two general approaches for developing a non-ergodic GMM with a GP regression. In the first approach, which was followed by Landwehr et al. (2016), all the coefficients, ergodic and non-ergodic, were modeled as GPs. In that case, the non-ergodic GMM is developed from the beginning and the response variable is typically the log of the ground-motion parameter (e.g. $\ln(PSA)$). An alternative approach, which was followed by Kuehn (2021a) and Lavrentiadis et al. (2021), is to model the non-ergodic coefficients or non-ergodic coefficient adjustments as GPs and keep the ergodic terms fixed. Here, the non-ergodic GMM is based on an existing ergodic GMM and the response variable is the ergodic residual. An advantage of this approach is that the extrapolation to large magnitudes and short distances from the underlying ergodic GMM is preserved in the non-ergodic GMM.

The remaining parts of this section summarize the different elements of the VCM GP GMM development: Bayesian regression, covariance functions of the prior distributions commonly used in VCM GP GMM, cell-specific anelastic attenuation, prediction of the median, and epistemic uncertainty of the non-ergodic coefficients and median ground motion at new locations.

5.1.1 Bayesian regression

In Bayesian statistics, the uncertainty of the model parameters and hyperparameters, θ and θ_{hyp} , before observing the data is expressed by the prior distribution ($p(\theta, \theta_{hyp})$). The uncertainty of θ and θ_{hyp} is updated based on the ground-motion observations, \mathbf{y} , and ground-motion parameters (such as M, R_{rup}, V_{S30} , etc., collectively for all records noted as \mathbf{x}) to produce the posterior distribution ($p(\theta, \theta_{hyp} | \mathbf{y}, \mathbf{x})$). The Bayes theorem provides the means for this calculation:

$$p(\theta, \theta_{hyp} | \mathbf{y}, \mathbf{x}) = \frac{\mathcal{L}(\theta, \theta_{hyp})p(\theta, \theta_{hyp})}{p(\mathbf{y}, \mathbf{x})} \tag{10}$$

Often, the normalizing distribution $p(\mathbf{y}, \mathbf{x})$ is omitted for computational efficiency as it is not required to sample or compute the maximum of the posterior. In this case the posterior distribution is expressed as:

$$p(\theta, \theta_{hyp} | \mathbf{y}, \mathbf{x}) \propto \mathcal{L}(\theta, \theta_{hyp})p(\theta, \theta_{hyp}) \tag{11}$$

The influence of the ground-motion data in the posterior distribution is expressed through the likelihood function ($\mathcal{L}(\boldsymbol{\theta}, \boldsymbol{\theta}_{hyp})$) — it corresponds to the likelihood (i.e probability) of observing the data given some values for $\boldsymbol{\theta}$ and $\boldsymbol{\theta}_{hyp}$. The likelihood for a single observation can be estimated with the functional form of the GMM as:

$$\mathcal{L}(\boldsymbol{\theta}, \boldsymbol{\theta}_{hyp}) = pdf(y|f_{nerg}(\mathbf{x}, \boldsymbol{\theta}, \boldsymbol{\theta}_{hyp}) + \delta\mathbf{B}_e^0, \phi_0^2) \tag{12}$$

Because all correlated terms (i.e. non-ergodic terms and between event residuals) are included in the mean, the misfit: $y - (f_{nerg}(\mathbf{x}, \boldsymbol{\theta}, \boldsymbol{\theta}_{hyp}) + \delta\mathbf{B}_e^0)$, which corresponds to δWS_{es}^0 , is independently and identically distributed, thus, the joint likelihood of all observations is the product of the likelihoods of individual observations:

$$\begin{aligned} \mathcal{L}(\boldsymbol{\theta}, \boldsymbol{\theta}_{hyp}) &= pdf(y|f_{nerg}(\mathbf{x}, \boldsymbol{\theta}, \boldsymbol{\theta}_{hyp}) + \delta\mathbf{B}_e^0, \phi_0^2) \\ &= \prod_{e=1}^{n_e} \prod_{s=1}^{n_s} pdf(y_{es}|f_{nerg}(x_{es}, \boldsymbol{\theta}, \boldsymbol{\theta}_{hyp}) + \delta\mathbf{B}_e^0, \phi_0^2) \end{aligned} \tag{13}$$

improving computational efficiency. The likelihood function is written in vector notation in the first line and expanded in the second line of Equation 13.

The prior distributions express our knowledge and beliefs about $\boldsymbol{\theta}$ and $\boldsymbol{\theta}_{hyp}$. They may come from prior experience in building non-ergodic GMMs or based on a desired model behavior (i.e. penalize model complexity if not supported by the data (Simpson et al. 2017)). When there is little information about $\boldsymbol{\theta}$ and $\boldsymbol{\theta}_{hyp}$, weakly informative priors can be used. These are chosen as wide priors distributions so that the posterior distribution is primarily controlled by the likelihood function.

The prior distributions of the non-ergodic effects are spatially uniform with zero means and large standard deviations because prior to interrogating the ground-motion data, the systematic effects are unknown. With the aid of the likelihood function and ground-motion data, the non-ergodic effects can be estimated close to stations and past earthquake locations. This results in posterior distributions that are spatially varying with non-zero means and smaller standard deviations where the non-ergodic effects have been estimated. Zero posterior standard deviations would imply that the non-ergodic effects are known with absolute certainty.

Historically, Bayesian inference has seen limited use due to its high computational cost compared to point-estimate inference with MLE. However, in recent years, with the increase in computational speed, Bayesian models have been gaining wider adoption. There are three main computationally-tractable approaches to obtain the posterior distributions of complex models that do not have analytical solutions; they are summarized below.

The maximum a posteriori (MAP) approach finds the values of $\boldsymbol{\theta}$ and $\boldsymbol{\theta}_{hyp}$ that correspond to the mode of the posterior. The posterior distribution is proportional to the product of the likelihood function and the prior distribution (Eq. 11). MAP can be found by minimizing the negative of this product, which can be computed easily numerically with gradient-based methods. In this sense, MAP is equivalent to a penalized MLE where the prior distribution acts as a regularization on the likelihood function. MAP is computationally faster than the other numerical solutions of Bayesian models, but its main shortcoming is that it provides a point estimate not the entire posterior distribution; thus, the uncertainty of the model cannot be assessed. The GPML toolbox (Rasmussen and Nickisch 2010) available in Matlab and Octave provides such MAP estimates for Gaussian Process models.

The Markov Chain Monte Carlo (MCMC) approach generates samples from the posterior distributions that are used in the inference of $\boldsymbol{\theta}$ and $\boldsymbol{\theta}_{hyp}$. This approach is able to recreate the full posterior distribution, but it is computationally slow. An in-depth review

of this method can be found at Brooks et al. (2011). Widely used statistical software that have implemented this approach are: JAGS (Plummer 2003), BUGS (Lunn et al. 2009), and STAN (Stan Development Team 2019) for general Bayesian models, and GPflow (van der Wilk et al. 2020) in Python for GPs.

A more recent approach consists in using approximation methods to compute the posterior distributions of θ and θ_{hyp} . These approximation solutions are applicable to specific families of Bayesian models. One such approximation method is the integrated nested Laplace approximation, INLA (Rue et al. 2009); it uses the Laplace approximation to efficiently compute the approximations to the marginal posterior distributions of Latent Gaussian Models (LGMs). In this family of models, the response variable is expressed as an additive function of the model parameters ($y = \sum_{i=1}^n \theta_i x_i$), and all θ_i follow Normal prior distributions. INLA is a useful approximation for developing GMMs as both ergodic GMMs and non-ergodic VCM GP GMMs can be formulated as LGMs. Further information regarding the INLA approximation can be found in Krainski et al. (2019, 2021) and Wang et al. (2018). A primer for developing ergodic GMMs with INLA can be found in Kuehn (2021a).

Other methods for Bayesian regression include the Variational Inference (Blei et al. 2017) which approximates the posterior distribution with a member of a closed-form probability distribution.

5.1.2 Covariance functions

The covariance functions, or kernel functions as often called in the literature, of the prior distributions are a crucial ingredient of the GP regression. They impose a correlation structure which dictates how a random variable (i.e. a coefficient or the ground-motion intensity parameter) varies in space. The covariance functions described in this section are isotropic and stationary; that is, the size and rate of spatial variation they impose is independent of the direction and location. Although this is likely a simplification for the systematic ground-motion effects, most of the non-ergodic GMM of this special issue did not use non-stationary and anisotropic kernel functions due to their additional computational challenge. Ground-motion studies that used non-stationary correlation structures include Kuehn and Abrahamson (2020) and Chen et al. (2021). Other studies that applied non-stationary and anisotropic correlation structures to GP regressions include Paciorek and Schervish (2006) and Finley (2011).

The four covariance functions described here are: the identity kernel function, the spatially independent kernel function, the constant kernel function, and the exponential kernel function. Examples, where these covariance functions are combined to create more complex spatial correlation structures, are provided at the end of this section. The covariance matrices, which are used in the regression and prediction of GP, are created by evaluating the covariance functions at all indices, such as the earthquake or station IDs, or coordinate pairs, such as the earthquake or station coordinates:

$$\mathbf{K}_{ikl} = \kappa_i(t_k, t_l) \quad (14)$$

where κ_i and \mathbf{K}_i are the covariance function and covariance matrix for the i^{th} coefficient, and t_k and t_l are the k^{th} and l^{th} indices or coordinate values. Indices are used as input to the kernel function if the correlation structure of the i^{th} coefficient depends on information such as the event or station number, while coordinates are used as input if the correlation

structure depends on information like the event or site location. In vector notation the covariance matrix is defined as:

$$\mathbf{K}_i = \kappa_i(\mathbf{t}, \mathbf{t}') \tag{15}$$

where \mathbf{t} and \mathbf{t}' are index or coordinate arrays. If \mathbf{K}_i is used in the regression phase, \mathbf{t} and \mathbf{t}' correspond to the existing scenarios; these are the scenarios in the regression dataset. However, if \mathbf{K}_i is used in the prediction phase, \mathbf{t} and \mathbf{t}' correspond to combinations of the existing and new scenarios. Further details on the GP prediction are provided in Sect. 5.1.4.

The identity kernel function is given by:

$$\kappa_i(t_k, t_l) = \omega_i^2 \delta(k - l) \tag{16}$$

where $\delta(x)$ is the Dirac delta function ($\delta(x = 0) = 1$ and $\delta(x \neq 0) = 0$). It is used for random variables that are statistically independent with ω being the standard deviation of the normal distribution. It generates a covariance matrix that is equal to ω^2 along the diagonal and zero everywhere else. This kernel function is used to model the within-event within-site aleatory term, δWS_{es} .

The spatially independent kernel function is given by:

$$\kappa_i(t_k, t_l) = \omega_i^2 \delta(\|t_k - t_l\|) \tag{17}$$

This kernel imposes perfect correlation between random variables at the same location or with the same index, and zero correlation between random variables at different locations or with different indices. The hyper-parameter ω defines the size of the variability, that is, how much the values of the random variable vary between points that are not collocated. If t_k and t_l are pair of coordinates, $\|t_k - t_l\|$ corresponds to the L2 distance norm (i.e. Euclidean distance) between the two coordinates. If t_k and t_l are indices, $\|t_k - t_l\|$ corresponds to the absolute difference between the two values.

Depending on the software, the covariance matrix of a spatially independent non-ergodic term can be modeled either with the identity or spatially independent kernel function. For example, consider a spatially independent site term, $\delta c_{i,S}$, that has a unique value at every site but zero spatial correlation. If a statistical software requires all terms to be of size N , where N is the number of records, the spatially independent kernel function should be used. That is because, if k^{th} and l^{th} recording have the same station coordinates, $\delta c_{i,S,k}$ and $\delta c_{i,S,l}$ should be equal (i.e. perfectly correlated). In this approach, all covariance matrices are size $N \times N$. However, if a statistical software can model terms of different sizes, the identity kernel function can be used. In this case, it is more efficient to estimate $\delta c_{i,S}$ at unique station locations and then pass it to the associated recordings. In this approach, $\delta c_{i,S}$ is uncorrelated, as every station coordinate is repeated only once, thus it can be modeled with an identity covariance matrix of size $N_s \times N_s$, where N_s is the number of stations, reducing the and number of operations and memory requirements.

The constant kernel function is given by:

$$\kappa_i(t_k, t_l) = \omega_i^2 \tag{18}$$

with ω controlling the deviation from the mean of the prior distribution. It imposes perfect correlation between all random variables so that they all have the same offset from the mean function. As an example, in Landwehr et al. (2016), the constant kernel function was applied to all coefficients to model their deviation from the mean of the prior which was equal to zero.

Alternatively, constant offsets in the coefficients can be modeled with a one-dimensional prior distribution on the mean function of the coefficient, as in the case of $\mathbf{c}_{\alpha,p}$ in Lavrentiadis et al. (2021). It depends on the modeler and software which option is more attractive. The main advantage of the first option is that it includes all information in the kernel function, while the main advantage of the second option is that it can lead to a sparse covariance matrix.

The exponential kernel function is given by:

$$\kappa_i(t_k, t_l) = \omega_i^2 e^{-\frac{\|t_k - t_l\|}{\ell_i}} \quad (19)$$

This kernel function is applied to spatially varying random variables. The hyperparameters ℓ and ω control the specific length scale and size of the spatial variation. At the two extremes of ℓ , the exponential kernel converges to a spatially independent and constant kernel function. For $\ell \rightarrow 0^+$ the spatial correlation weakens converging to a spatially independent kernel function, while for $\ell \rightarrow +\infty$ the correlation becomes stronger converging to a constant kernel function. With this kernel function, a random variable is assumed to vary continuously but not smoothly in space (i.e. the spatial variation of the random variable is continuous, but the first derivative of the spatial variation is not). This kernel function is widely used in geostatistics to model spatially varying phenomena.

Another kernel function for modeling continuously spatially varying random variables is the squared exponential. This kernel function is infinitely differentiable resulting in very smooth spatial variations that may be unrealistic for spatial processes (Stein 1991). However, the main advantage of this covariance function is that it is separable in the X and Y coordinates which allows for efficient approximations of the kernel function for large datasets (Lacour 2022).

More complex correlation structures can be built by combining the kernel functions described above using the properties of the Normal distribution. For example, assume a non-ergodic site adjustment $\delta c_{i,S}$ that is the combined effect of an underlying continuous adjustment over large distances and a site-specific adjustment. Such a site adjustment can be broken into individual components: $\delta c_{ia,S}$ for the underlying continuous adjustment, and $\delta c_{ib,S}$ for site-specific adjustment, with $\delta c_{i,S} = \delta c_{ia,S} + \delta c_{ib,S}$. In this case, $\delta c_{ia,S}$ can be assigned a prior distribution which has a zero prior mean and an exponential kernel function ($\kappa_{ia,S}$), and $\delta c_{ib,S}$ can be assigned a prior distribution which has a zero prior mean and a spatially-independent kernel function ($\kappa_{ib,S}$):

$$\begin{aligned} \delta c_{ia,S} &\sim \mathcal{N}(\mathbf{0}, \kappa_{ia,S}(t_S, t'_S)) \\ \delta c_{ib,S} &\sim \mathcal{N}(\mathbf{0}, \kappa_{ib,S}(t_S, t'_S)) \end{aligned} \quad (20)$$

Based on the linear properties of the Normal distribution, the prior distribution of $\delta c_{i,S}$ has a mean which is equal to the sum of mean functions of the individual components, and a kernel function which is equal to the sum of the kernel functions of the individual components:

$$\delta c_{i,S} \sim \mathcal{N}(\mathbf{0}, \kappa_{ia,S}(t_S, t'_S) + \kappa_{ib,S}(t_S, t'_S)) \quad (21)$$

Similarly, the kernel function of the median non-ergodic ground motion can be obtained by combining the kernel functions of the GMM coefficients. For simplicity, only three terms of the ergodic base GMM (Eq. 1) are used in this example:

$$f_{nerg} = c_1 + c_{4,E}(t_E) \ln(R_{eff}) + c_{10,S}(t_S) \ln(V_{S30}/V_{ref}) \tag{22}$$

where $R_{eff} = R + c_6$, c_1 is the intercept, $c_{4,E}$ is the geometrical-spreading term which is a function of the earthquake coordinates and scales with $\ln(R_{eff})$, and $c_{10,S}$ is a linear site amplification term which is a function of the site coordinates and scales with $\ln(V_{S30}/V_{ref})$.

If, the GMM coefficients are modeled as GPs with prior distributions:

$$\begin{aligned} c_1 &\sim \mathcal{N}(\boldsymbol{\mu}_1, \boldsymbol{\kappa}_1) \\ c_{4,E} &\sim \mathcal{N}(\boldsymbol{\mu}_{4,E}, \boldsymbol{\kappa}_{4,E}(t_E, t'_E)) \\ c_{10,S} &\sim \mathcal{N}(\boldsymbol{\mu}_{10,S}, \boldsymbol{\kappa}_{10,E}(t_S, t'_S)) \end{aligned} \tag{23}$$

with $\boldsymbol{\mu}_i$ and $\boldsymbol{\kappa}_i$ being the mean and kernel functions of the i^{th} coefficient, respectively; the prior distribution of f_{nerg} is equal to:

$$\begin{aligned} \mathbf{f}_{nerg} &\sim \mathcal{N}\left(\boldsymbol{\mu}_1 + \boldsymbol{\mu}_{4,E} \ln(\mathbf{R}_{eff}) + \boldsymbol{\mu}_{10,S} \ln(\mathbf{V}_{S30}/\mathbf{V}_{ref}), \right. \\ &\quad \boldsymbol{\kappa}_1 + \boldsymbol{\kappa}_{4,E}(t_E, t'_E) \circ (\ln(\mathbf{R}_{eff}) \ln(\mathbf{R}_{eff})^T) \\ &\quad \left. + \boldsymbol{\kappa}_{10,S}(t_S, t'_S) \circ (\ln(\mathbf{V}_{S30}/\mathbf{V}_{ref}) \ln(\mathbf{V}_{S30}/\mathbf{V}_{ref})^T)\right) \end{aligned} \tag{24}$$

in which the symbol \circ corresponds to the element-wise product, and $\ln(\mathbf{R}_{eff})$ and $\ln(\mathbf{V}_{S30}/\mathbf{V}_{ref})$ are column vectors with the $\ln(R_{eff})$ and $\ln(V_{S30}/V_{ref})$ values of all recordings. A linear combination of Normal distributions follows a Normal distribution. The mean of f_{nerg} is equal to the linear combination of the means of the prior distributions of the coefficients. To get a more intuitive feeling for the kernel function of f_{nerg} , first consider the covariance between just two scenarios $cov(f_{nergk}, f_{nerg l})$. By substituting Eq. 22 into the covariance and assuming the coefficients of the GMM are independent with each other ($cov(c_i, c_j) = 0$ if $i \neq j$) we obtain:

$$\begin{aligned} cov(f_{nergk}, f_{nerg l}) &= cov(c_1, c_1) \\ &+ \ln(R_{effk}) cov(c_{4,E}(t_{Ek}), c_{4,E}(t_{El})) \ln(R_{eff l}) \\ &+ \ln(V_{S30k}) cov(c_{10,S}(t_{Sk}), c_{10,S}(t_{Sl})) \ln(V_{S30 l}) \\ &= \boldsymbol{\kappa}_1 + \ln(R_{effk}) \boldsymbol{\kappa}_{4,E}(t_{Ek}, t_{El}) \ln(R_{eff l}) \\ &+ \ln(V_{S30k}/V_{ref}) \boldsymbol{\kappa}_{10,S}(t_{Sk}, t_{Sl}) \ln(V_{S30 l}/V_{ref}) \end{aligned} \tag{25}$$

The kernel function in Eq. 24 creates the same covariance as Eq. 25 for all recordings. For example, for the $c_{1,S}$ contribution, the $\ln(\mathbf{R}_{eff}) \ln(\mathbf{R}_{eff})^T$ product creates a matrix with all $\ln(R_{effk}) \ln(R_{eff l})$ permutations, and the element-wise product with $\boldsymbol{\kappa}_4(t_E, t'_E)$ combines these permutations with the covariance of the coefficient.

Generalizing from previous example, the covariance function of the median ground motion between scenarios k and l is:

$$\boldsymbol{\kappa}_{nergkl} = \sum_{i=1}^d x_{ik} \boldsymbol{\kappa}_i(t_{ik}, t_{il}) x_{il} \tag{26}$$

in which $\boldsymbol{\kappa}_{nerg}$ is the kernel function for f_{nerg} , $\boldsymbol{\kappa}_i$ is the kernel function of the i^{th} non-ergodic coefficient, x_i is the independent variable in front of the i^{th} non-ergodic coefficient (e.g. $\ln(R_{eff})$), t_i is input coordinate or ID for $\boldsymbol{\kappa}_i$, and d is the number of the non-ergodic terms.

In matrix notation Eq. 26 can be defined as:

$$\kappa_{nerg} = \sum_{i=1}^d \kappa_i(t_i, t'_i) \circ (x_i, x_i^T) \tag{27}$$

5.1.3 Cell-specific anelastic attenuation

The cell-specific anelastic attenuation was first proposed by Dawood and Rodriguez-Marek (2013) and then extended by Kuehn et al. (2019) and Abrahamson et al. (2019) as an approach to capture the systematic effects related to the paths. In this method, the domain of interest is divided into a grid of cells and each cell is assigned its own anelastic attenuation. For each recording, the ray path that connects a point on the rupture with the site is broken into cell-path segments (ΔR_i) which are the lengths of the ray within each cell (Fig. 2). For a given recording, the total anelastic attenuation can be calculated by $f_{atten,P} = c_{ca,P} \cdot \Delta R$ where $c_{ca,P}$ is vector containing the attenuation coefficients of all the cells.

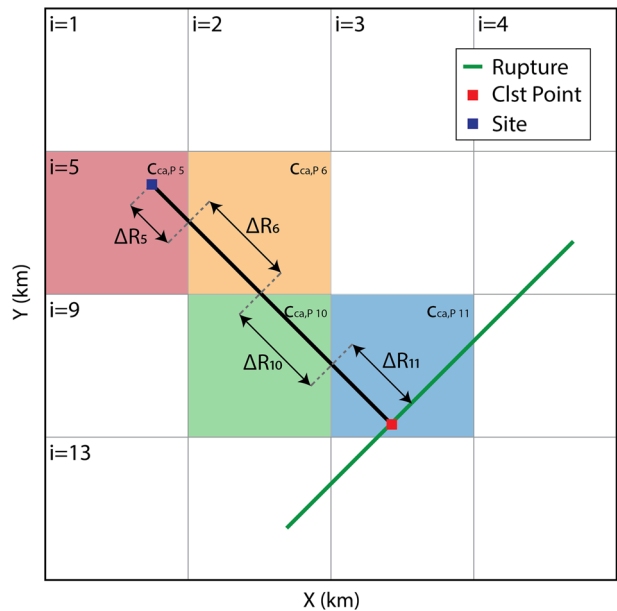
Currently, there is no consensus on the origin point for the ray path. Dawood and Rodriguez-Marek (2013) used the epicenter, while Kuehn et al. (2019) and Lavrentiadis et al. (2021) used the closest point on the rupture to the site, as the length of that path is equal to R_{rup} , which is a common distance metric for anelastic attenuation in ergodic GMMs. Additional research is needed in this area to test different options for the origin of the ray path and also investigate if there is any magnitude dependence in the location of the representative point for finite-fault ruptures.

In GP, the cell attenuation can be modeled similarly to the other spatially varying non-ergodic terms using a Truncated Normal as a prior distribution:

$$c_{ca,P} \sim \mathcal{N}(\mu_{ca,P}, \kappa_{ca,P}(t_C, t'_C)) \mathcal{T}(, 0) \tag{28}$$

the cell attenuation is limited to be equal or less than zero to ensure the proper extrapolation of the GMM. In statistical software that does not include truncated Normal distributions,

Fig. 2 Schematic showing the calculation of the cell-path segments for the cell-specific anelastic attenuation. $c_{ca,P}$ is the anelastic attenuation coefficient and ΔR_i is the cell-path segment of the i^{th} cell



the cell-specific attenuation is modeled with a Normal prior, but at a postprocessing step it is checked that no or only a small number of cells have positive attenuation.

The mean of the prior distribution, $\mu_{ca,P}$, controls the average anelastic attenuation of the cells, while the kernel function, $\kappa_{ca,P}$, controls their spatial correlation. In regions with sparse coverage, the cell-specific anelastic attenuation is close to $\mu_{ca,P}$ as there are not enough data to inform the posterior. In regions with significant coverage, the cell-specific anelastic attenuation deviates from $\mu_{ca,P}$ to capture the systematic path effects which influence the ground motion in those regions. The $\mu_{ca,P}$ can be either fixed to the anelastic attenuation of the ergodic GMM or be assigned its own prior distribution. The second option is computationally more involved but takes into account the re-weighting of the paths. In an ergodic GMM, the anelastic attenuation is controlled by the attenuation of the areas with high-path coverage; however, in the cell-specific anelastic attenuation, the mean attenuation is determined at the cell level, the path coverage controls the mean and epistemic uncertainty of the individual cells, but it does not have a direct impact on the mean attenuation of all cells, which is why the mean of the cell-specific anelastic attenuation and the ergodic anelastic attenuation can be different.

The kernel functions that were presented in Sect. 5.1.2 can also be used to model the spatial correlation of the cell attenuation. For instance, Kuehn et al. (2019) used the spatially independent kernel function, while Lavrentiadis et al. (2021) used a combination of the exponential and spatially independent kernel function. Other approaches for modeling the spatial correlation of cell-specific anelastic attenuation are the conditional autoregressive (CAR) and simultaneous autoregressive (SAR) models (Ver Hoef et al. 2018). These models have sparse precision matrices (i.e. inverse of covariance matrices) reducing the computational cost.

The prior distribution for the total anelastic attenuation can be derived from the prior distribution for the cell attenuation using the linear transformation properties of the Normal distribution:

$$f_{atten,P} \sim \mathcal{N}(\Delta\mathbf{R} \mu_{ca,P}, \Delta\mathbf{R} \kappa_{ca,P}(t_C, t'_C) \Delta\mathbf{R}^T) \mathcal{I}(0) \tag{29}$$

where $\Delta\mathbf{R}$ is a matrix with the cell-path segments of all recordings, the i^{th} row of $\Delta\mathbf{R}$ is equal to $\Delta\mathbf{R}$ of the i^{th} recording. The $f_{atten,P}$ prior distribution can be used in GP to make direct predictions for the median non-ergodic ground motion at new locations (Sect. 5.1.4).

5.1.4 Prediction

The median non-ergodic ground motion can be predicted for the new scenarios either by first predicting the non-ergodic coefficients and then substituting them at the non-ergodic functional form or by predicting the non-ergodic ground motion directly. This choice depends on how the GPs are modeled. If the GMM terms are modeled as GPs explicitly, the first method is used. However, if the GMM terms are modeled as GPs implicitly (i.e. they have been integrated out in the likelihood function), the second method is used.

5.1.4.1 Prediction of non-ergodic coefficients The non-ergodic coefficient adjustments for the new scenarios can be predicted based on the hyperparameters and posterior distribution of the coefficient adjustments of the existing scenarios. Initially, we consider the case where the non-ergodic coefficient adjustments of the existing scenarios have zero epistemic uncertainty. The joint prior distribution between the non-ergodic coefficient adjustments of the existing and new scenarios is:

$$\begin{bmatrix} \delta c_i \\ \delta c_i^* \end{bmatrix} \sim \mathcal{N}\left(\begin{bmatrix} \mathbf{0} \\ \mathbf{0} \end{bmatrix}, \begin{bmatrix} \mathbf{K}_i & \mathbf{k}_i \\ \mathbf{k}_i^T & \mathbf{K}_i^* \end{bmatrix}\right) \tag{30}$$

in which δc_i are the non-ergodic coefficient adjustments of the existing scenarios, δc_i^* are the non-ergodic coefficient adjustments of new scenarios, \mathbf{K}_i is the prior covariance between all pairs of existing scenarios ($\mathbf{K}_{ijkl} = \kappa_i(t_k, t_l)$), \mathbf{K}_i^* is the prior covariance between all pairs of new scenarios ($\mathbf{K}_{ijkl}^* = \kappa_i(t_k^*, t_l^*)$), and \mathbf{k}_i is the prior covariance between all pairs of existing and new scenarios ($\mathbf{k}_{ijkl} = \kappa_i(t_k, t_l^*)$).

Because of the cross-correlation between the non-ergodic coefficient adjustments of the existing and new scenarios, described by \mathbf{k} , the posterior distributions of δc_i^* can be predicted by ensuring that they are in agreement with δc_i . A naive approach for that would be to generate multiple realizations of δc_i^* from the joint prior distribution (Eq. 30) and reject those that are inconsistent with δc_i . The distribution of the accepted realizations δc_i^* would correspond to the posterior distribution of δc_i^* . Although this is theoretically correct, it would be computationally inefficient. In statistics, this can be performed easily by conditioning δc_i^* on δc_i , which corresponds to predicting δc_i^* based on the values of δc_i . The conditional distribution of a joint Normal prior distribution is also a Normal distribution:

$$\delta c_i^* | \delta c_i \sim \mathcal{N}(\boldsymbol{\mu}_{\delta c_i^* | \delta c_i}, \boldsymbol{\Psi}_{\delta c_i^* | \delta c_i}) \tag{31}$$

with $\boldsymbol{\mu}_{\delta c_i^* | \delta c_i}$ and $\boldsymbol{\Psi}_{\delta c_i^* | \delta c_i}$ being the mean and covariance of the posterior distributions of δc_i^* given by (Rasmussen and Williams 2006):

$$\boldsymbol{\mu}_{\delta c_i^* | \delta c_i} = \mathbf{k}_i^T \mathbf{K}_i^{-1} \delta c_i \tag{32}$$

$$\boldsymbol{\Psi}_{\delta c_i^* | \delta c_i} = \mathbf{K}_i^* - \mathbf{k}_i^T \mathbf{K}_i^{-1} \mathbf{k}_i \tag{33}$$

In other fields where GP regression is used, one is typically interested only in the point-wise uncertainty which means that the mean and epistemic uncertainty of δc_i^* can be calculated independently for each scenario reducing the computational cost. However, in PSHA it is necessary to calculate the full covariance for the new scenarios, as the spatial correlation of δc_i^* , which described by the off-diagonal term of $\boldsymbol{\Psi}_{\delta c_i^* | \delta c_i}$, needs to be included in the logic tree.

A more realistic case is for there to be some uncertainty in the estimation of the non-ergodic coefficient adjustments of the existing scenarios described by the posterior distribution ($p(\delta c_i | \mathbf{y}, \mathbf{x})$). This uncertainty can be propagated in the prediction of the non-ergodic coefficient adjustments of the new scenarios by predicting δc_i^* using all possible values of δc_i and considering how likely each δc_i is ($p(\delta c_i | \mathbf{y}, \mathbf{x})$). In statistics, this is defined as marginalization of δc_i^* :

$$p(\delta c_i^* | \mathbf{y}, \mathbf{x}) = \int p(\delta c_i^* | \delta c_i) p(\delta c_i | \mathbf{y}, \mathbf{x}) d\delta c_i \tag{34}$$

where the probability density function $p(\delta c_i^* | \delta c_i)$ can be obtained from the conditional distribution in Eq. 31.

A closed-form solution for the posterior distribution of δc_i^* which includes the uncertainty of δc_i can be obtained if the posterior distribution of δc_i is assumed to be Normal (Lavrentiadis et al. 2021):

$$\delta c_i | y, x \sim \mathcal{N}(\mu_{\delta c_i | y, x}, \Psi_{\delta c_i | y, x}) \tag{35}$$

where $\mu_{\delta c_i | y, x}$ is the mean, and $\Psi_{\delta c_i | y, x}$ is the covariance of the posterior distribution of δc_i . With this assumption, Eq. 34 results in a Normal distribution:

$$\delta c_i^* | y, x \sim \mathcal{N}(\mu_{\delta c_i^* | y, x}, \Psi_{\delta c_i^* | y, x}) \tag{36}$$

with the mean and covariance given in Eqs. (37) and (38), respectively (Bishop 2006).

$$\mu_{\delta c_i^* | y, x} = \mathbf{k}_i^T \mathbf{K}_i^{-1} \mu_{\delta c_i | y, x} \tag{37}$$

$$\Psi_{\delta c_i^* | y, x} = \mathbf{K}_i^* - \mathbf{k}_i^T \mathbf{K}_i^{-1} \mathbf{k}_i + \mathbf{k}_i^T \mathbf{K}_i^{-1} \Psi_{\delta c_i | y, x} (\mathbf{k}_i^T \mathbf{K}_i^{-1})^T \tag{38}$$

The assumption that the posterior distribution of δc_i is Normal is considered reasonable because in a GP regression all non-ergodic terms have Normal prior distributions. If the hyperparameters are fixed or follow Normal prior distributions, this assumption would be absolutely valid; however, because some of the hyperparameters are assigned different prior distributions, the posterior distribution of δc_i may slightly deviate from this assumption. For the prediction of δc_i^* , Kuehn (2021b) showed that this approximation gives consistent results with Eq. 34 where the full posterior distribution of δc_i is used.

The non-ergodic coefficients of the new scenarios (c_i^*) can be computed similarly to δc_i^* , however, the non-zero prior means needs to be considered:

$$\mu_{\delta c_i^* | y, x} = \mathbf{k}_i^T \mathbf{K}_i^{-1} (\mu_{\delta c_i | y, x} - \mu_{\delta c_i}) + \mu_{\delta c_i^*} \tag{39}$$

$$\Psi_{\delta c_i^* | y, x} = \mathbf{K}_i^* - \mathbf{k}_i^T \mathbf{K}_i^{-1} \mathbf{k}_i + \mathbf{k}_i^T \mathbf{K}_i^{-1} \Psi_{\delta c_i | y, x} (\mathbf{k}_i^T \mathbf{K}_i^{-1})^T \tag{40}$$

where $\mu_{\delta c_i}$ and $\mu_{\delta c_i^*}$ are the prior means of the non-ergodic coefficients for the existing and new scenarios.

Prediction of non-ergodic ground motion

An alternative approach to predict the median non-ergodic ground motion for the new scenarios, f_{nerg}^* , is to directly obtain it from the ground-motion observations of the exciting scenarios, y (Landwehr et al. 2016). The main difference between this approach and the previous approach is that y includes an aleatory component which must be considered in the predictions. The joint prior distribution between ground-motion observations of the existing scenarios and median non-ergodic ground motion of the new scenarios is:

$$\begin{bmatrix} y \\ f_{nerg}^* \end{bmatrix} \sim \mathcal{N} \left(\begin{bmatrix} \mu_f \\ \mu_f^* \end{bmatrix}, \begin{bmatrix} \mathbf{K}_f + \phi_0^2 \mathbf{I} + \tau_0^2 \mathbf{1} & \mathbf{k}_f \\ \mathbf{k}_f^T & \mathbf{K}_f^* \end{bmatrix} \right) \tag{41}$$

where μ_f is the prior mean of the ground-motion of the existing scenarios, and μ_f^* is the prior mean of the ground-motion of the new scenarios. The \mathbf{K}_f , \mathbf{K}_f^* , and \mathbf{k}_f are the prior covariance for the epistemic uncertainty of the ground-motion between all pairs of existing, new, and existing/new scenarios, respectively, and $\phi_0^2 \mathbf{I}$ and $\tau_0^2 \mathbf{1}$ are the covariance for the within-event and between-event aleatory variability.

The μ_f and μ_f^* depend on how the non-ergodic GMM is being developed. If it is based on a backbone ergodic model, μ_f and μ_f^* are equal to f_{erg} for the existing and new scenarios. That is, without any knowledge of the non-ergodic effects, both the mean of the observations and non-ergodic ground motion are equal to the means the ergodic ground

motion. However, if the non-ergodic GMM is developed from the beginning, $\boldsymbol{\mu}_f$ and $\boldsymbol{\mu}_f^*$ are equal to zero.

The prior covariance for the epistemic uncertainty of the ground motion can be obtained by combining the kernel functions of the non-ergodic coefficients as shown in Sect. 5.1.2, $\mathbf{K}_{fkl} = \sum_{i=1}^d x_{ik} \boldsymbol{\kappa}_i(t_{ik}, t_{il}) x_{il}$. Similarly, $\mathbf{K}_{fkl}^* = \sum_{i=1}^d x_{ik}^* \boldsymbol{\kappa}_i(t_{ik}^*, t_{il}^*) x_{il}^*$, and $\mathbf{k}_{fkl} = \sum_{i=1}^d x_{ik} \boldsymbol{\kappa}_i(\mathbf{t}_k, \mathbf{t}_l^*) x_{il}^*$. The prior covariance for \mathbf{y} includes $\phi_0^2 \mathbf{I}$ and $\tau_0^2 \mathbf{I}$ because the deviation of ground-motion observations from $\boldsymbol{\mu}_f$ is the result of both aleatory variability and epistemic uncertainty. There is not aleatory variability in covariance between the ground-motion observations of the existing scenarios and the mean ground-motion of the new scenarios as any correlation between the two comes from the systematic non-ergodic terms. Similarly, the covariance of \mathbf{f}_{nerg}^* does not include an aleatory component, as it corresponds to the median prediction of the non-ergodic ground motion.

Once the joint prior distribution is defined, the median non-ergodic ground motion can be predicted by expressing it as a conditional distribution on the ground-motion observations:

$$\mathbf{f}_{nerg}^* | \mathbf{y} \sim \mathcal{N}(\boldsymbol{\mu}_{f_{nerg}^* | \mathbf{y}}, \boldsymbol{\Psi}_{f_{nerg}^* | \mathbf{y}}) \tag{42}$$

with the mean and the covariance of the conditional distribution given in Eqs. 43 and 44.

$$\boldsymbol{\mu}_{f_{nerg}^* | \mathbf{y}} = \boldsymbol{\mu}_f^* + \mathbf{k}_f^T (\mathbf{K}_f + \phi_0^2 \mathbf{I} + \tau_0^2 \mathbf{I})^{-1} (\mathbf{y} - \boldsymbol{\mu}_f) \tag{43}$$

$$\boldsymbol{\Psi}_{f_{nerg}^* | \mathbf{y}} = \mathbf{K}_f^* - \mathbf{k}_f^T (\mathbf{K}_f + \phi_0^2 \mathbf{I} + \tau_0^2 \mathbf{I})^{-1} \mathbf{k}_f \tag{44}$$

5.2 Model extrapolation constraints and epistemic uncertainty

In developing any type of GMM—ergodic or non-ergodic—attention must be paid to its proper extrapolation. That is because GMMs are typically derived on datasets primarily composed of small-to-moderate earthquakes at medium-to-large distances, but in PSHA, they are applied to large earthquakes at short distances. For that, the trends in the dataset are insufficient to guide the extrapolation of a GMM and additional constraints need to be introduced.

These constraints can be imposed both on the model parameters as well as the model hyperparameters. Two common constraints for the model parameters are related to the magnitude saturation at short distances and anelastic attenuation.

Full magnitude saturation at short distances means that, close to the fault, the ground motion does not scale with magnitude. Similarly, over saturation with magnitude means that, close to the fault, the ground motions reduce as the magnitude increases. This is a controversial issue because empirical datasets, such as NGAWest2, show trends of oversaturation for large magnitudes at short periods and small distances, but the results of numerical simulations support positive magnitude scaling (Collins et al. 2006; Abrahamson and Silva 2007). Due to the limited number of empirical data from large events, and practical design purposes most GMMs do not allow oversaturation and impose full saturation as a lower limit on the regressions. One such practical consideration is that, if oversaturation is allowed, a structure would need to be designed not only for the largest magnitude but for the smaller events too as they could lead to higher seismic demands. This is straightforward to model in PSHA, but it becomes more complicated when selecting conservative deterministic scenarios.

In a GMM, the magnitude saturation of short periods at zero distance from the rupture is controlled by the combination of the linear magnitude scaling coefficient, the geometrical

spreading coefficient, the magnitude scaling coefficient for the geometrical spreading, and the pseudo-depth coefficient in geometrical spreading. In the example GMM provided in Eq. 1, the coefficients control magnitude saturation are: c_2 , c_5 and c_6 . Full magnitude saturation at zero distance is achieved by:

$$c_5 = \frac{-c_2}{\ln(c_6)} \quad (45)$$

With this functional form, it is easy to derive a non-ergodic GMM with a full saturation constraint, as the c_2 , c_5 , and c_6 coefficients are treated as fixed terms. However, it may be more difficult to impose this constraint with other common functional forms. For example, Chiou and Youngs (2014) (CY14) uses a different functional form, and full saturation is achieved by:

$$c_2 = -c_4 c_6 \quad (46)$$

where c_2 is the linear magnitude scaling, c_4 is the near-source geometrical spreading, and c_6 controls the magnitude dependence of the geometrical spreading. In this functional form, it is harder to include a spatially varying non-ergodic geometrical spreading as the value of c_4 would also affect the magnitude saturation. A non-ergodic GMM developer should consider factors like this when deciding on the functional form and statistical software to use.

The anelastic attenuation is intended to capture the reduction of the amplitude of the seismic waves due to the dissipation of energy as they travel through the earth's crust; thus, the anelastic attenuation coefficient or cell-specific anelastic attenuation must be negative to make physical sense. However, it should be noted that due to the correlation between the linear distance term and the geometrical spreading term, the physical interpretation of the linear distance term as anelastic attenuation depends on using a realistic geometrical spreading term. Similarly to the magnitude saturation, the GMM developer should either use statistical methods and software that allows them to impose an appropriate constraint on these terms, or if that is not feasible to ensure that the model has reasonable distance scaling when used in forward calculations.

Constraints can also be applied to hyperparameters to impose a desired model behavior. For instance, if a VCM GMM contains both a spatially varying site constant and a spatially varying V_{S30} coefficient as a function of the site coordinates, it may be deemed reasonable to constrain the correlation length of the site constant to be smaller than the correlation length of the V_{S30} coefficient. That is because, the repeatable effects related to the site amplification due to the underlying geologic structure, which the V_{S30} intends to model, are broader than the repeatable effects related to the site-specific site amplification. Additionally, such a constraint will limit any trade-offs between the two coefficients as they would capture systematic site effects at different length scales.

The epistemic uncertainty of a non-ergodic GMM quantifies the confidence in estimating the systematic source, path, and site effects; however, it does not quantify the confidence in the model extrapolation. The latter is typically expressed by the model-to-model epistemic uncertainty, which reflects the range of scientifically defensible approaches for developing a GMM. In PSHA, this uncertainty is typically captured either by using multiple GMMs or by shifting the median estimate of a base GMM. As an example of the second approach, Abrahamson et al. (2019) incorporated the model-to-model epistemic uncertainty into a non-ergodic PSHA study for California by estimating the epistemic uncertainty and correlation of the coefficients of a common GMM functional based on the NGAWest2 GMMs and propagating them into the ground-motion prediction.

Another source of model-to-model epistemic uncertainty for non-ergodic GMM is related to the different statistical approaches and decisions in modeling the non-ergodic terms. For example, different covariance functions (e.g. exponential, squared exponential) can be used to model the spatially varying non-ergodic terms or even entirely different modeling approaches (e.g. GP regression, ANNs). Such choices are expected to lead to bigger differences in areas with sparse data.

Different intensity measures are affected differently by magnitude scaling. *PSA*, especially at short periods, is sensitive to the entire frequency content of the ground motion (i.e. spectral shape). This can be an issue when developing a GMM predominately with small earthquakes as their frequency content is different from the frequency content of large events which are more common in PSHA, potentially resulting in incorrect scaling coefficients. A solution to this is developing a GMM for an intermediary intensity parameter (*IP*) that is not sensitive to spectral shape and using a transformation to convert the prediction to *PSA*. One such example is Lavrentiadis and Abrahamson (2021) where used *EAS* was used as an intermediary *IP* and Random vibration theory was used to convert *EAS* to *PSA*.

5.3 Other methods for non-ergodic models

The previous sections provided an in-depth discussion on developing non-ergodic GMMs using Gaussian process. Although it has many useful properties, it is not the only method for developing non-ergodic GMMs. This section provides a brief review of other methods that have been used for this task.

Sung and Lee (2019) built more than 700 single-station GMMs for the Taiwan region. Single-station GMMs do not include non-ergodic site terms, instead, they are independently regressed with ground motions recorded at a single station. Kriging interpolation is used to estimate the spatial distributions of the single-station GMM coefficients and aleatory terms at new locations. This is a simpler approach for developing a partially non-ergodic GMM, but it cannot provide estimates of the epistemic uncertainty at the new locations as VCM GP GMM does.

Caramenti et al. (2020) used a multi-source geographically-weighted regression (MS-GWR) to develop a non-ergodic GMM for Italy. It is similar to GP in that the spatial correlation of the non-ergodic terms is also captured through kernel functions; however, it is more efficient as it is based on the least-squares regression. The main shortcoming of this approach is that the aleatory variability is described by a single term so it is unable to capture the correlation between the recordings of the same earthquake.

Okazaki et al. (2021) developed a single-station GMM for *PGA* using an ANN trained on strong-motion data from the KiK-net seismograph network in Japan. In this study, the systematic site effects were expressed as a function of site ID and estimated through the ANN fitting.

6 Concluding remarks

A summary of different methods for the development of non-ergodic GMMs is presented in this paper. An emphasis is placed on methods that use GP as it offers a convenient framework for expressing spatially varying non-ergodic terms. The cell-specific anelastic attenuation can be combined with GP to model systematic effects related to the path. A simple example of the steps for developing a non-ergodic GMM using a synthetic dataset and making predictions at new locations is included in the electronic supplement.

The use of non-ergodic GMMs in PSHA is a promising development, as the reduction in aleatory variability can have a large impact on the seismic hazard at large return periods, and improve the accuracy of the site-specific hazard. In PSHA applications, the reduction of the aleatory variability should be combined with the change in the epistemic uncertainty due to the uncertainty in the estimates of the non-ergodic terms in addition to the epistemic uncertainty in the extrapolation to large magnitudes and short distances of the underlying ergodic GMMs. There is a higher computational cost associated with the development and application of non-ergodic GMMs. This limitation can be overcome by utilizing high-performance computers or efficient approximation methods. For example, INLA (Rue et al. 2009) provides an efficient method for estimating the non-ergodic terms, and Lacour and Abrahamson (2019) provide an efficient approach for propagating non-ergodic effects in PSHA. Additionally, there is an ongoing effort by the Natural Hazards Risk and Resiliency Research Center at the Garrick Institute for the Risk Sciences at the University of California, Los Angeles to verify various software packages for developing non-ergodic GMMs which is expected to facilitate the adoption of non-ergodic GMMs. The results of that effort will be published in the near future.

As larger datasets become available, new non-ergodic GMMs are anticipated to continue adding spatially varying non-ergodic terms to capture more systematic site, path, and source effects. With this, non-ergodic GMMs will start to mimic the spatial resolution of numerical simulations with 3-D crustal structures. Numerical simulations can also be used to test the decisions and assumptions associated with non-ergodic GMM scaling (Meng and Goulet, In press). There is still uncertainty in the repeatability of source effects for a given region or for a single fault. In particular, with the use of small magnitude events to constrain the non-ergodic terms, the scaling of the non-ergodic source terms from small magnitudes to larger magnitudes has not been validated. The variability due to fault physics complexity may inherently be irreducible at the time scales we are working with, even in consideration of fault maturity information, which is quite limited. In that case, non-ergodic GMMs will have a limited improvement in the accuracy of source effects. Similarly, path effects constrained by small events are theoretically simpler than for large events (waves emitted from different points of the fault and traversing a large volume to a site where their effect is aggregated). Developments in three key areas can improve non-ergodic modeling: (a) earthquake physics to help with better prediction of source effects, (b) numerical simulations to quantify the differences in path effects of large earthquakes with extended ruptures and small earthquakes with point source ruptures, and (c) continued collection of recorded motions to further constrain repeatable effects over large areas. Future studies should also evaluate the stability of hyperparameters between different areas to determine if a set of generic hyperparameters can be used. This will allow the development of non-ergodic GMM for regions with fewer recordings, as larger datasets are required to estimate the model hyperparameters than to estimate non-ergodic terms. Finally, even in consideration of their current limitations, non-ergodic GMMs such as those described here have advantages over ergodic (or global) GMMs in increasing the accuracy of PSHA estimates and are expected to remain a useful tool to this end.

7 Glossary of proposed notation

7.1 Acronyms

IP	Intensity parameter
PSA	Pseudo spectral acceleration
FAS	Fourier amplitude spectra
EAS	Effective amplitude spectra
GMM	Ground motion model
VCM	Varying coefficient model
MLE	Maximum likelihood estimation
GP	Gaussian Process
RVT	Random vibration theory

7.2 GMM input variables

M	Moment magnitude
R_{rup}	Closest distance to the rupture plane
R_x	Horizontal distance from the top of the rupture measured perpendicular to the fault strike
R_{y0}	Horizontal distance off the end of the rupture measured parallel to strike.
ΔR	Cell-path segments lengths of the anelastic attenuation cells
V_{S30}	Time average shear wave velocity at the top 30m
V_{ref}	Reference V_{S30} for the linear site amplification
z_{1100}	Depth to 1100m/sec shear-wave velocity
Dip	Fault dip angle.
F_{RV}	Reverse fault scaling factor
F_N	Normal fault scaling factor
f_{NL}	Non-linear site amplification
f_{HW}	Hanging wall scaling

7.3 Model parameters

c_i	Ergodic GMM coefficient
$c_{i,X}$	Non-ergodic GMM coefficient where X can be S for systematic site effects, P for systematic site effects, or E for systematic site source
$\delta c_{i,X}$	Non-ergodic adjustment to GMM coefficient
$c_{ca,P}$	Cell specific anelastic attenuation coefficients
$\delta S2S$	Total site-to-site non-ergodic term
$\delta P2P$	Total path-to-path non-ergodic term
$\delta L2L$	Total Source-to-source non-ergodic term
δB_e	Between-event aleatory term

δW_{es}	Within-event aleatory terms
δWS_{es}	Within-event within-site term of a partially non-ergodic GMM
δB_e^0	Between-event term of a non-ergodic GMM
δWS_{es}^0	Within-event within-site term of a non-ergodic GMM

7.4 Model hyperparameters

$\ell_{i,X}$	Correlation length in the kernel function of $c_{i,X}$ or $\delta c_{i,X}$
$\omega_{i,X}$	Scale/Standard deviation of the $c_{i,X}$ or $\delta c_{i,X}$ kernel function
ϕ_{S2S}	Standard deviation of $\delta S2S$
ϕ_{P2P}	Standard deviation of $\delta P2P$
τ_{L2L}	Standard deviation of $\delta L2L$
τ	Standard deviation of δB_{es}
ϕ	Standard deviation of $\delta W_{e,s}$
τ_0	Standard deviation of δB_e^0
ϕ_0	Standard deviation of $\delta WS_{e,s}^0$

7.5 Other symbols

y	Response variable of GMM
x	Array of GMM input variables (e.g. R_{rup} , V_{S30})
ρ	Correlation coefficient
θ	Array of all GMM parameters
θ_{hyp}	Array of all GMM hyperparameters
$\kappa_i(t, t')$	Kernel function of $c_{i,x}$ or $\delta c_{i,x}$
t_E	Earthquake coordinates
t_{Rup}	Coordinates of the closest-point on the rupture to each site
t_S	Site coordinates
t_{MP}	Coordinate of mid-point between source and site
t_C	Cell coordinates
$\mu(y)$	Mean estimate of the y ground-motion parameter
$\psi(y)$	Epistemic uncertainty of y ground-motion parameter
$\mu(c_i)$	Mean estimate of c_i coefficient
$\psi(c_i)$	Epistemic uncertainty of c_i coefficient
$\hat{*}$	New scenarios in GP predictions (e.g. t_E^* corresponds to location of new earthquake)
f_{erg}	Median ergodic ground motion function.
f_{nerg}	Median non-ergodic ground motion function.

Acknowledgements This study was supported by the Pacific Gas and Electric Company and the California Department of Transportation. Any opinions, findings, and conclusions or recommendations expressed in this material are those of the authors and do not necessarily reflect those of the sponsoring agencies. Constructive comments on an early draft of this manuscript provided by Linda Al Atik, Morgan P. Moschetti, Niels Landwehr, Franklin R. Olaya, and Kyle B. Withers are gratefully appreciated. The authors are also thankful to Jack W. Baker for the review and constructive comments that helped to improve the final article.

Funding Partial funding for this study has been provided by the Pacific Gas and Electric Company and California Department of Transportation

Declarations

Conflict of interest The authors declare that they have no conflict of interest.

Ethics approval Non applicable

Consent to participate Non applicable

Consent for publication Non applicable

Code availability A series of tools for developing and applying non-erodic VCM GP GMM are provided at: https://github.com/NHR3-UCLA/ngmm_tools

Open Access This article is licensed under a Creative Commons Attribution 4.0 International License, which permits use, sharing, adaptation, distribution and reproduction in any medium or format, as long as you give appropriate credit to the original author(s) and the source, provide a link to the Creative Commons licence, and indicate if changes were made. The images or other third party material in this article are included in the article's Creative Commons licence, unless indicated otherwise in a credit line to the material. If material is not included in the article's Creative Commons licence and your intended use is not permitted by statutory regulation or exceeds the permitted use, you will need to obtain permission directly from the copyright holder. To view a copy of this licence, visit <http://creativecommons.org/licenses/by/4.0/>.

References


- Abrahamson NA, Silva WJ (2007) Abrahamson and Silva NGA Ground Motion Relations for the Geometric Mean Horizontal Component of Peak and Spectral Ground Motion Parameters. Tech. rep, PEER, Berkeley, CA
- Abrahamson NA, Youngs RR (1992) A stable algorithm for regression analyses using the random effects model. *Bull Seismol Soc Am* 82(1):505–510. <http://www.bssaonline.org/content/82/1/505.short>
- Abrahamson NA, Silva WJ, Kamai R (2014) Summary of the ASK14 ground motion relation for active crustal regions. *Earthq Spectra* 30(3):1025–1055. <https://doi.org/10.1193/070913EQS198M>
- Abrahamson NA, Al-Atik L, Bayless J, Dinsick A, Dreger DS, Gregor N, Kuehn N, Walling M, Watson-Lamprey J, Wooddell K, Youngs RR (2015) Southwestern united states ground motion characterization sshac level 3. Tech. rep., GeoPentech, rev. 2
- Abrahamson NA, Kuehn NM, Walling M, Landwehr N (2019) Probabilistic Seismic Hazard Analysis in California Using Nonergodic Ground Motion Models. *Bulletin of the Seismological Society of America* 109(4):1235–1249. <https://doi.org/10.1785/0120190030>. <https://pubs.geoscienceworld.org/ssa/bssa/article/109/4/1235/571959/>
- Al Atik L, Abrahamson NA, Bommer JJ, Scherbaum F, Cotton F, Kuehn NM (2010) The variability of ground-motion prediction models and its components. *Seismol Res Lett* 81(5):794–801 <https://doi.org/10.1785/gssrl.81.5.794>. <https://pubs.geoscienceworld.org/srl/article/81/5/794-801/143735>
- Ancheta TD, Darragh RB, Stewart JP, Seyhan E, Silva WJ, Chiou BS, Wooddell KE, Graves RW, Kottke AR, Boore DM, Kishida T, Donahue JL (2014) NGA-West2 database. *Earthq Spectra* 30(3):989–1005. <https://doi.org/10.1193/070913EQS197M>
- Anderson JG, Brune JN (1999) Probabilistic seismic hazard analysis without the ergodic assumption. *Seismol Res Lett* 70(1):19–28. <https://doi.org/10.1785/gssrl.70.1.19>
- Arroyo D, Ordaz M (2010) Multivariate Bayesian regression analysis applied to ground-motion prediction equations, part 1: theory and synthetic example. *Bull Seismol Soc Am* 100(4):1551–1567. <https://doi.org/10.1785/0120080354>
- Arroyo D, Ordaz M (2010) Multivariate Bayesian regression analysis applied to ground-motion prediction equations, part 2: numerical example with actual data. *Bull Seismol Soc Am* 100(4):1568–1577. <https://doi.org/10.1785/0120090320>

- Bates D, Mächler M, Bolker B, Walker S (2015) Fitting linear mixed-effects models using lme4. *J Stat Softw* 67(1), 1–48, <https://doi.org/10.18637/jss.v067.i01>
- Bishop CM (2006) *Pattern recognition and machine learning*. Springer, New York, NY
- Blei DM, Kucukelbir A, McAuliffe JD (2017) Variational inference: a review for statisticians. *J Am Stat Assoc* 112(518):859–877. <https://doi.org/10.1080/01621459.2017.1285773>
- Brooks S, Gelman A, Jones G, Meng XL (2011) *Handbook of Markov Chain Monte Carlo*, vol 148. Chapman and Hall/CRC <https://doi.org/10.1201/b10905>. <https://www.taylorfrancis.com/books/9781420079425>
- Caramenti L, Menafoglio A, Sgobba S, Lanzano G (2020) Multi-source geographically weighted regression for regionalized ground-motion models. Tech. Rep. 67/2020, MOX, Dipartimento di Matematica Politecnico di Milano, Milano, Italy
- Chen Y, Bradley BA, Baker JW (2021) Nonstationary spatial correlation in New Zealand strong ground-motion data. *Earthq Eng Struct Dyn*. <https://doi.org/10.1002/eqe.3516>
- Chiou BS, Youngs RR (2014) Update of the Chiou and Youngs NGA model for the average horizontal component of peak ground motion and response spectra. *Earthq Spectra* 30(3):1117–1153, <https://doi.org/10.1193/072813EQS219M>. <http://earthquakespectra.org/doi/10.1193/072813EQS219M>
- Collins N, Graves R, Somerville P (2006) Revised analysis of 1d rock simulations for the NGA-e project. Tech. rep, PEER, Berkeley, CA
- Dawood HM, Rodriguez-Marek A (2013) A Method for including path effects in ground-motion prediction equations: an example using the Mw 9.0 Tohoku earthquake aftershocks. *Bull Seismol Soc Am* 103(2B):1360–1372. <https://doi.org/10.1785/0120120125>
- Der Kiureghian A, Ditlevsen O (2009) Aleatory or epistemic? Does it matter? *Struct Saf* 31(2):105–112. <https://doi.org/10.1016/j.strusafe.2008.06.020>
- Derras B, Bard PY, Cotton F (2014) Towards fully data driven ground-motion prediction models for Europe. *Bull Earthq Eng* 12(1):495–516. <https://doi.org/10.1007/s10518-013-9481-0>
- Finley AO (2011) Comparing spatially-varying coefficients models for analysis of ecological data with non-stationary and anisotropic residual dependence. *Methods Ecol Evol* 2(2):143–154. <https://doi.org/10.1111/j.2041-210X.2010.00060.x>
- Hermkes M, Kuehn NM, Riggelsen C (2014) Simultaneous quantification of epistemic and aleatory uncertainty in GMPEs using Gaussian process regression. *Bull Earthq Eng* 12(1):449–466. <https://doi.org/10.1007/s10518-013-9507-7>
- Krainski E, Gómez-Rubio V, Bakka H, Lenzi A, Castro-Camilo D, Simpson D, Lindgren F, Rue H (2019) Advanced spatial modeling with stochastic partial differential equations using R and INLA. Chapman and Hall/CRC. <https://doi.org/10.1201/9780429031892>. <https://www.taylorfrancis.com/books/9780429629853>
- Krainski E, Gómez-Rubio V, Bakka H, Lenzi A, Castro-Camilo D, Simpson D, Lindgren F, Rue H (2021) Advanced spatial modeling with stochastic partial differential equations using R and INLA. <https://becar.ioprecario.bitbucket.io/spde-gitbook/>
- Kuehn N (2021a) A primer for using INLA to estimate ground-motion models. Tech. rep. <https://doi.org/10.31224/osf.io/6ut3p>. <https://engrxiv.org/6ut3p/>
- Kuehn N (2021b) Comparison of bayesian varying coefficient models for the development of nonergodic ground-motion models. *Bull Earthq Eng*
- Kuehn NM, Abrahamson NA (2018) The effect of uncertainty in predictor variables on the estimation of ground–motion prediction equations. *Bull Seismol Soc Am* 108(1):358–370. <https://doi.org/10.1785/0120170166>. <https://pubs.geoscienceworld.org/ssa/bssa/article/108/1/358/523092/The-Effect-of-Uncertainty-in-Predictor-Variables>
- Kuehn NM, Abrahamson NA (2020) Spatial correlations of ground motion for non-ergodic seismic hazard analysis. *Earthquake Eng Struct Dynam* 49(1):4–23. <https://doi.org/10.1002/eqe.3221>
- Kuehn NM, Abrahamson NA, Walling MA (2019) Incorporating nonergodic path effects into the NGA–West2 ground–motion prediction equations. *Bull Seismol Soc Am* 109(2):575–585. <https://doi.org/10.1785/0120180260>. <https://pubs.geoscienceworld.org/ssa/bssa/article/569193/Incorporating-Nonergodic-Path-Effects-into-the>
- Kuehn NM, Kishida T, AlHamaydeh M, Lavrentiadis G, Bozorgnia Y (2020) A Bayesian model for truncated regression for the estimation of empirical ground-motion models. *Bull Earthq Eng* 18(14):6149–6179. <https://doi.org/10.1007/s10518-020-00943-8>
- Lacour M (2022) Efficient non-ergodic ground-motion prediction for large datasets. *Bull Earthq Eng*. <https://doi.org/10.1007/s10518-022-01402-2>
- Lacour M, Abrahamson NA (2019) Efficient propagation of epistemic uncertainty in the median ground–motion model in probabilistic hazard calculations. *Bull Seismol Soc Am* 109(5):2063–2072. <https://doi.org/10.1785/0120180327>. <https://pubs.geoscienceworld.org/ssa/bssa/article/109/5/2063/572186/Efficient-Propagation-of-Epistemic-Uncertainty-in>

- Landwehr N, Kuehn NM, Scheffer T, Abrahamson NA (2016) A nonergodic ground-motion model for California with spatially varying coefficients. *Bull Seismol Soc Am* 106(6):2574–2583. <https://doi.org/10.1785/0120160118>
- Lavrentiadis G (2021) Non-ergodic ground-motion models for California, Ground-motion embedment factors for the Seattle Region, and Global fault displacement model. University of California, Berkeley
- Lavrentiadis G, Abrahamson NA (2021) A non-ergodic spectral acceleration ground motion model for California developed with random vibration theory. arXiv preprint [arXiv:2107.09125](https://arxiv.org/abs/2107.09125)
- Lavrentiadis G, Abrahamson NA, Kuehn NM (2021) A non-ergodic effective amplitude ground-motion model for California. *Bull Earthq Eng* (0123456789). <https://doi.org/10.1007/s10518-021-01206-w>. <https://link.springer.com/10.1007/s10518-021-01206-w>
- Lin PS, Chiou BS, Abrahamson NA, Walling M, Lee CT, Cheng CT (2011) Repeatable source, site, and path effects on the standard deviation for empirical ground-motion prediction models. *Bull Seismol Soc Am* 101(5):2281–2295. <https://doi.org/10.1785/0120090312>
- Lunn D, Spiegelhalter D, Thomas A, Best N (2009) The BUGS project: Evolution, critique and future directions. *Stat Med* 28(25):3049–3067. <https://doi.org/10.1002/sim.3680>. <https://onlinelibrary.wiley.com/doi/10.1002/sim.3680>
- Meng X, Goulet C (In press) Lessons learned from applying varying coefficient model to controlled simulation datasets. *Bull Earthq Eng*
- Okazaki T, Morikawa N, Iwaki A, Fujiwara H, Iwata T, Ueda N (2021) Ground-motion prediction model based on neural networks to extract site properties from observational records. *Bull Seismol Soc Am* 111(4):1740–1753. <https://doi.org/10.1785/0120200339>
- Ordaz M, Singh SK, Arciniega A (1994) Bayesian attenuation regressions: an application to Mexico City. *Geophys J Int* 117(2):335–344. <https://doi.org/10.1111/j.1365-246X.1994.tb03936.x>
- Paciorek CJ, Schervish MJ (2006) Spatial modelling using a new class of nonstationary covariance functions. *Environmetrics* 17(5):483–506. <https://doi.org/10.1002/env.785>
- Plummer M (2003) JAGS : A Program for Analysis of Bayesian Graphical Models Using Gibbs Sampling JAGS : Just Another Gibbs sampler. In: DSC 2003 working papers, Vienna, Austria. <http://www.ci.tuwien.ac.at/Conferences/DSC-2003/>
- Powell MJ (2009) The Bobyqa algorithm for bound constrained optimization without derivatives. Cambridge NA Report NA2009/06, University of Cambridge, Cambridge 26
- R Core Team (2020) R: A Language and Environment for Statistical Computing. R Foundation for Statistical Computing, Vienna, Austria. <https://www.R-project.org/>
- Rasmussen CE, Nickisch H (2010) Gaussian processes for machine learning (GPML) toolbox. *J Mach Learn Res* 11:3011–3015
- Rasmussen CE, Williams CKI (2006) Gaussian processes for machine learning. The MIT Press, Cambridge, pp 715–719
- Rue H, Martino S, Chopin N (2009) Approximate Bayesian inference for latent Gaussian models by using integrated nested Laplace approximations. *J R Stat Soc Ser B Stat Methodol* 71(2):319–392. <https://doi.org/10.1111/j.1467-9868.2008.00700.x>
- Simpson D, Rue H, Riebler A, Martins TG, Sørbye SH (2017) Penalising model component complexity: a principled, practical approach to constructing priors. *Stat Sci* 32(1):1–28. <https://doi.org/10.1214/16-STS576>
- Stan Development Team (2019) The Stan Core Library. <http://mc-stan.org/>, version 2.25.0
- Stein ML (1991) A kernel approximation to the kriging predictor of a spatial process. *Ann Inst Stat Math* 43(1):61–75. <https://doi.org/10.1007/BF00116469>
- Stewart JP, Afshari K, Goulet CA (2017) Non-ergodic site response in seismic hazard analysis. *Earthq Spectra* 33(4):1385–1414. <https://doi.org/10.1193/081716EQS135M>
- Sung CH, Lee CT (2019) Improvement of the quantification of epistemic uncertainty using single-station ground-motion prediction equations. *Bull Seismol Soc Am* 109(4):1358–1377
- Trugman DT, Shearer PM (2018) Strong correlation between stress drop and peak ground acceleration for recent M 1–4 earthquakes in the San Francisco bay area. *Bull Seismol Soc Am* 108(2):929–945. <https://doi.org/10.1785/0120170245>
- van der Wilk M, Dutordoir V, John S, Artemev A, Adam V, Hensman J (2020) A framework for interdomain and multioutput Gaussian processes. [arXiv:2003.01115](https://arxiv.org/abs/2003.01115). <https://arxiv.org/abs/2003.01115>
- Ver Hoef JM, Peterson EE, Hooten MB, Hanks EM, Fortin MJ (2018) Spatial autoregressive models for statistical inference from ecological data. *Ecol Monogr* 88(1):36–59. <https://doi.org/10.1002/ecm.1283>
- Wang X, Ryan YY, Faraway JJ (2018) Bayesian regression modeling with INLA. Chapman & Hall/CRC, Boca Raton
- Withers KB, Moschetti MP, Thompson EM (2020) A machine learning approach to developing ground motion models from simulated ground motions. *Geophys Res Lett* 47(6):1–9. <https://doi.org/10.1029/2019GL086690>

Publisher's Note Springer Nature remains neutral with regard to jurisdictional claims in published maps and institutional affiliations.

Authors and Affiliations

Grigorios Lavrentiadis¹  · Norman A. Abrahamson² · Kuehn M. Nicolas¹ · Yousef Bozorgnia³ · Christine A. Goulet⁴ · Anže Babič⁵ · Jorge Macedo⁶ · Matjaž Dolšek⁵ · Nicholas Gregor⁷ · Albert R. Kottke⁸ · Maxime Lacour⁹ · Chenying Liu⁶ · Xiaofeng Meng⁴ · Van-Bang Phung¹⁰ · Chih-Hsuan Sung¹⁰ · Melanie Walling¹¹

Norman A. Abrahamson
abrahamson@berkeley.edu

Kuehn M. Nicolas
kuehn@ucla.edu

Yousef Bozorgnia
yousef.bozorgnia@ucla.edu

Christine A. Goulet
cgoulet@usc.edu

Anže Babič
ababic@fgg.uni-lj.si

Jorge Macedo
jorge.macedo@gatech.edu

Matjaž Dolšek
mdolsek@fgg.uni-lj.si

Nicholas Gregor

Albert R. Kottke
albert.kottke@pge.com

Maxime Lacour
maxlacour@berkeley.edu

Chenying Liu
cliu662@gatech.edu

Xiaofeng Meng
xiaofenm@usc.edu

Van-Bang Phung
bangntu01@gmail.com

Chih-Hsuan Sung
karensung@berkeley.edu

Melanie Walling
mwalling@geoengineers.com

¹ Natural Hazards Risk and Resiliency Research Center (NHR3), Garrick Institute for the Risk Sciences University of California, Los Angeles Boelter Hall 4825, Los Angeles, CA 90095-1593, USA

² Department of Civil Engineering, University of California, Berkeley, 455 Davis Hall, Berkeley, CA 94720, USA

- ³ Natural Hazards Risk and Resiliency Research Center (NHR3), Garrick Institute for the Risk Sciences University of California, Los Angeles Boelter Hall 4731-C, Los Angeles, CA 90095-1593, USA
- ⁴ Southern California Earthquake Center, University of Southern California, Zumberge Hall of Science 3651 Trousdale Pkwy, Los Angeles, CA 90089, USA
- ⁵ Faculty of Civil and Geodetic Engineering, University of Ljubljana, Jamova cesta 2, Ljubljana, Slovenia
- ⁶ School of Civil and Environmental Engineering, Georgia Institute of Technology, 790 Atlantic Drive, Atlanta, GA 30332-0355, USA
- ⁷ 32 Camellia Place, Oakland, CA 94602, USA
- ⁸ Geosciences Pacific Gas and Electric Co., 300 Lakeside Drive, Oakland, CA 94612, USA
- ⁹ Department of Civil and Environmental Engineering, University of California, Berkeley, 450 Davis Hall, Berkeley, CA 94720, USA
- ¹⁰ Department of Civil and Environmental Engineering, University of California, Berkeley, 409 Davis Hall, Berkeley, CA 94720, USA
- ¹¹ Performance-Based Risk Assessment, GeoEngineers, Inc., 17425 NE Union Hill Road Ste 250, Redmond, WA 98052, USA